



HAL
open science

Preparation of bactericidal PDMS surfaces by benzophenone photo-initiated grafting of polynorbornenes functionalized with quaternary phosphonium or pyridinium groups

Yuzhen Lou, Damien Schapman, Dimitri Mercier, N. Ceren Süer, Tarik Eren, Pascal Thebault, Nasreddine Kébir

► To cite this version:

Yuzhen Lou, Damien Schapman, Dimitri Mercier, N. Ceren Süer, Tarik Eren, et al.. Preparation of bactericidal PDMS surfaces by benzophenone photo-initiated grafting of polynorbornenes functionalized with quaternary phosphonium or pyridinium groups. *European Polymer Journal*, 2021, 157, pp.110669. 10.1016/j.eurpolymj.2021.110669 . hal-03612244

HAL Id: hal-03612244

<https://hal.science/hal-03612244>

Submitted on 2 Aug 2023

HAL is a multi-disciplinary open access archive for the deposit and dissemination of scientific research documents, whether they are published or not. The documents may come from teaching and research institutions in France or abroad, or from public or private research centers.

L'archive ouverte pluridisciplinaire **HAL**, est destinée au dépôt et à la diffusion de documents scientifiques de niveau recherche, publiés ou non, émanant des établissements d'enseignement et de recherche français ou étrangers, des laboratoires publics ou privés.



Distributed under a Creative Commons Attribution - NonCommercial 4.0 International License

Preparation of bactericidal PDMS surfaces by benzophenone photo-initiated grafting of polynorbornenes functionalized with quaternary phosphonium or pyridinium groups

Yuzhen Lou¹, Damien Schapman², Dimitri Mercier³, N. Ceren Sürer⁴, Tarik Eren⁴, Pascal Thebault⁵, Nasreddine Kébir¹

¹ Normandie Université, INSA Rouen Normandie, Laboratoire PBS, UMR CNRS 6270 & FR 3038, Avenue de l'Université, 76801 Saint Etienne du Rouvray, France

² Normandie Université, UNIROUEN, IFR MP 23, PRIMACEN, 76821 Mont-Saint-Aignan, France

³ PSL Research University, Chimie ParisTech – CNRS, Institut de Recherche de Chimie Paris, 11 rue Pierre et Marie Curie, 75005 Paris, France

⁴ Department of Chemistry, Yildiz Technical University, Davutpasa Campus, 34220, Esenler, Istanbul, Turkey

⁵ Normandie Université, UNIROUEN, laboratoire PBS, UMR CNRS 6270 & FR 3038, 76821 Mont-Saint-Aignan, France

Abstract

Cationic ROMP-polymers bearing ammonium or phosphonium groups were photo-grafted onto a PDMS surface via the thiol-ene click reaction, in the presence of benzophenone. The PDMS surface was first thiolated using pentaerythritol tetrakis (3-mercaptopropionate) (PTTMP) under UV, in the presence of benzophenone. The obtained cationic surfaces exhibited charge densities above 10^{14} charge/cm² and a higher degree of hydrophilicity compared to non-grafted surfaces. The live and dead tests performed by fluorescence microscopy revealed an effective contact bactericidal effect of these surfaces against *Escherichia coli* and *Staphylococcus epidermidis*.

Keywords: Quaternary ammonium; ROMP; photo; grafting to; PDMS; bactericidal; thiol-ene.

Corresponding authors: nasreddine.kebir@insa-rouen.fr ; pascal.thebault@univ-rouen.fr

Introduction

The increase of antibiotic-resistant microorganisms in recent years has become a crucial **issue**, which has spurred significant research efforts to develop more effective antimicrobial treatments that use different bactericidal mechanisms to neutralize infectious diseases [1]. While around 2.8 million cases of antibiotic-resistant infections occur each year in the United States. More than 35,000 of these cases result in death [2]. Cationic antimicrobial polymers represent a growing and evolving class of biocides as an alternative to existing biocides and antibiotics [3].

Since man-made materials are completely vulnerable to microbial growth, they can easily survive in a humid environment by attaching microbial cells to their surface. As the number of cells increases at the surface, they often begin to form a biofilm from a polysaccharide matrix with embedded cells. This formed biofilm allows microbial cells to survive under harsh conditions [4]. Unfortunately, embedded cells are up to 1,000 times less sensitive to most antibiotics and other biocides [5]. Moreover, many toxins expelled from biofilms make them pathogenic, and resistant infections spread [6]. Furthermore, there may be an exchange of antibiotic genes between bacteria within the biofilm, resulting in multiple resistant bacteria being combined [7].

Antimicrobial polymers show some advantages over existing biocides and are therefore becoming increasingly important in the surface area [8]. Cationic antimicrobial polymers generally show high activity, a broad-spectrum activity and have low resistance to build potential and reduced toxicity. These biocidal polymers can be physically affiliated onto **some** surfaces, **especially glass, which exhibit affinity with them**. Since antimicrobial polymers have high molecular weights and low diffusion coefficients, their leakage from **these** surfaces is restricted [9]. In addition, antimicrobial polymers can also be covalently bonded to surfaces, without losing their biological activity [10].

Polydimethylsiloxane (PDMS) is one of the most important polymer-based biomaterials. It is very flexible, chemically and thermally stable and biocompatible. It can be used in many different forms such as joint implants, catheters, kidney dialysis machines and breast prostheses [11]–[17]. Nevertheless, PDMS is a very hydrophobic material undergoing biofouling and bacterial contamination, which imply an important health and economic impacts [18]–[20].

One of the promising strategies to resolve these problems is the chemical anchoring of cationic antibacterial polymers onto the PDMS surface. However, because of its chemical

stability, the PDMS surface often needs a physical pretreatment to introduce coupling sites. For instance, oxygen plasma has been applied to create hydroxyl groups on the PDMS surface rendering it very hydrophilic [21]. Actually, in few minutes of contact with air, the surface hydroxyl groups diffuse in the polymer matrix bulk, which lead to hydrophobic recovery and the loss of surface functionalization. Therefore, the post-chemical grafting must be achieved just after the physical treatment [22].

Nowadays there is only two chemical pathways for the direct chemical modification of the PDMS surface [23]–[31]. The first one is the hydrosilylation reaction between Si-H groups present in the PDMS surface and carbon-carbon double bonds incorporated in bioactive polymers [23]–[28]. By varying the ratio between the PDMS components and/or their curing time or by insertion of poly(methylhydroxysiloxane), the concentration of Si-H groups can be fine-tuned [23]–[28]. The second one is the photo-induced ‘grafting from’ process of monomers or macromonomers, namely acrylic acid [29], polyethylene glycol monoacrylate, polyethylene glycol diacrylate [30], sulfobetaine methacrylate and carboxybetaine methacrylate [31], and vinylbenzyltrimethylbutylammonium chloride [32] from the PDMS surfaces, in the presence of benzophenone as photo-initiator.

In this work, we describe a straightforward photo-grafting of ROMP-synthesized bactericidal polynorbornenes bearing quaternary phosphonium (p(OPPh)) or pyridinium (p(OPyHex)) groups onto native and thiolated PDMS surfaces, in the presence of benzophenone. The physico-chemical and antimicrobial properties of the cationic surfaces are assessed and discussed with the literature data.

Experimental section

Materials

Sylgard[®] 184 was purchased from DOW chemical company (USA). Dry methanol (99,8%), acetone was purchased from Acros Organics. Glass coverslip (18 mm×18 mm, Fisherbrand[™]) were purchased from Thermo Fisher Scientific. Pentaerythritol tetrakis (3-mercaptopropionate) (PTTMP) was purchased from Aldrich. Benzophenone (BP) (≥99%) was purchased from Merck. Ultrapure water was obtained from a Milli-Q system (Siemens, France). All the chemicals were used without further purification.

S. epidermidis (ATCC 35984) and *E. coli* (K12 MG1655) strains were stored as frozen aliquots in brain heart infusion (BHI, Bacto, France) broth and 30 % of glycerol at -20 °C. The LIVE/DEAD Bacterial Viability Kit, L7007 (SYTO[®]9 dye, 1.67 mM / Propidium iodide,

18.3 mM) was purchased from Thermo Fisher Scientific. Phosphate buffered saline (PBS), prepared from the PBS tablets (Gibro, Swiss) and ultrapure water, was autoclaved before use.

Preparation of p(OPPh) and p(OPyHex)

The monomers and polymers with molecular weight of 10 000 g/mol used in the study were synthesized as described in the literature [33], [34].

Phosponium based monomer synthesis started with a Diels-Alder reaction between maleic anhydride and furan to obtain the starting compound of *exo*-7-oxabicyclo[2.2.1]hept-5-ene-2,3-dicarboxylic anhydride [35]. After that, imide transformation was conducted with 3-bromopropyl amine hydrobromide, according to the literature [36]. Bromo oxanorbornene product (0.5 g, 1.75 mmol) was dissolved in 11 mL of ethyl acetate. Excess amount of triphenylphosphine (1.376 g, 5.25mmol) was added to reaction medium. The reaction was stirred under nitrogen in a sealed vessel at 50 °C for 24 h. The precipitate of the reaction was washed with ethyl acetate and THF and dried under nitrogen.

Pyridinium based monomer was synthesized by the reaction of 3-(Aminomethyl)pyridine (2.4 mL, 22 mmol) and *exo*-7-oxabicyclo[2.2.1]hept-5-ene-2,3-dicarboxylic anhydride (1.92 g, 11 mmol) in the presence of 6 mL *N,N*-dimethylacetamide at 60 °C and stirred for 20 min. After addition of a catalytic amount of sodium acetate (0.5 g, 5 mmol) in 2 mL acetic anhydride to the solution, the reaction mixture was stirred for 2 h at 90 °C. The mixture was diluted with ethyl acetate, washed with brine and concentrated using a rotary evaporator connected to a vacuum pump. Product was purified by column chromatography using ethyl acetate:hexane (4:1, v/v). Quaternization of pyridine bearing oxanorbornene (0.13 g, 0.47 mmol) was obtained by using the bromohexane (0.67 g, 4.7 mmol) in the presence of acetonitrile solution stirred for 48 h at 60 °C, quaternized monomer was obtained by precipitation from diethyl ether.

For polymerization of p(OPPh), freshly prepared Grubbs third generation catalyst in 0.5 mL of dry dichloromethane was added in one shot to the forcibly stirring monomer solution in 2 mL dry chloroform and stirred for 24 h at room temperature. Afterwards the polymerization was stopped by addition of 0.5 mL 30 % ethylvinyl ether (in dichloromethane). Polymer, p(OPPh), was precipitated and washed with diethyl ether and dried under nitrogen.

For polymerization of OPyHex, the monomer was dissolved in dry methanol and after addition of Grubbs third generation catalyst dissolved in dichloromethane stirred for 2 hours.

All polymers were confirmed by thin layer chromatography (TLC) before the polymerization was terminated.

Preparation of PDMS film

15 g of a mixture of the two parts of Sylgard[®] 184, i.e. base and curing agent, at a ratio of 10:1 (w/w), were casted into a low-density polyethylene petri dish square (120×120×17 mm³). The mixture was then degassed under vacuum, until the air bubbles were completely removed. The PDMS film was formed after two days at room temperature and was cut into 18 × 18 mm² squares with a thickness less than 1 mm. The curing time can be considerably reduced by increasing the temperature (few hours at 70°C and about 1h at 120°C) [23].

Preparation of PDMS-T-p(OPPh) and PDMS-T-p(OPyHex) surfaces

To prepare PDMS-T, the PDMS films were first immersed in an acetone solution containing 20 wt% of BP for 30 min to absorb enough BP for the photo-grafting. The samples were quickly washed with methanol and then placed on a plate to dry in the dark. Then 50 to 80 µl of an acetone solution containing PTTMP (25 to 75wt%) was applied to the dry samples and covered with a glass slide so that the PTTMP solution was spread evenly over the surface of the PDMS by capillary force. The PDMS assembly was placed in a UV conveyor (UV Fusion Light Hammer 6), and irradiated with the UV light emitted from a small diameter electrodeless bulb combined with the elliptical reflector, microwave-powered lamp (500 watts/inch) at a lamp-PDMS distance of 53 mm. Then, the BP-initiated photo grafting and photopolymerization of the PTTMP took place from the PDMS surface. After grafting, PDMS-T were collected and washed in acetone overnight with slight shaking and washed again with acetone the next day before drying to remove all unreacted BP or PTTMP.

Then, PDMS-T-p(OPPh) or PDMS-T-p(OPyHex) were prepared by using the methanol solution containing p(OPPh) or p(OPyHex) in the same way on substrate of PDMS-T. After grafting, the samples were collected by immersion in water to detach from the glass slide and then washed with methanol three times. The samples were washed in methanol overnight with slight shaking and washed again with methanol the next day before vacuum drying to ensure that all unreacted monomer, ungrafted BP, p(OPPh) or p(OPyHex) compounds were removed.

Measurements

The ATR-FTIR spectra were recorded on a Nicolet IS-50 FTIR (Thermo, USA) spectrometer using the VariGATR accessory (Harrick Scientific, Pleasantville, NY) and the

DTGS detector on three independent samples for each experimental condition, with a wave-number range between 600 and 4000 cm^{-1} . The data was obtained with a spectral resolution of 4 cm^{-1} by 250 scans.

^1H NMR (500 MHz) and ^{13}C NMR (125 MHz) spectra were recorded on a Bruker Avance III 500 MHz spectrometer. ^{31}P NMR spectra were obtained using a Varian Mercury VX 400 MHz BB spectrometer.

Static and dynamic water contact angles measurements were measured using a contact angle goniometer “digidrop” (United Kingdom) in air at room temperature on at least three independent samples and at least three droplets by sample.

X-Ray Photoelectron spectroscopy (XPS) analysis was performed using a Thermo Electron Escalab 250 spectrometer, with a monochromatic Al $K\alpha$ X-ray source ($h\nu = 1486.6\text{eV}$) operating at a pressure around 10^{-9} mbar. The spectrometer was calibrated using Au4f7/2 at 84.1eV. The take-off angle was 90° and the analyzed surface was a 500 μm diameter disk. Survey spectra were recorded with a pass energy of 100eV and a step of 1eV and C1s, O1s, Si2p high level resolution spectra were recorded with a pass energy of 20eV and a step of 0.1eV. The charge effect was evaluated using the main component of the C1s peak, associated with C-C/C-H hydrocarbons with a binding energy of 285eV. Spectra were recorded using the Thermo Advantage software and analyzed using CasaXPS software.

The topography of PDMS surfaces before and after modification were analyzed by using a Nanoscope 8 Multimode microscope (Bruker Nano Surfaces, Santa Barbara, CA, USA). Imaging was achieved in the air using the PeakForce®-QNM mode with a 100 μm piezoelectric scanner. A silicon (RTESPA-300, Bruker) cantilever with a spring constant of about 40 N/m and a silicon tip was used. Images were obtained with a PeakForce tapping frequency of 1 kHz and the auto-amplitude on. The AFM imaging was performed in multiple locations on at least two independent samples at two scan sizes: 5×5 and $20 \times 20 \mu\text{m}^2$. All images are presented in the height mode and are top view images.

Determination of the surface accessible quaternary ammonium and phosphonium densities

Modified and unmodified PDMS surfaces ($1.8 \times 1.8 \text{ cm}^2$) were immersed in a solution of fluorescein sodium salt (1% in distilled water) for 10 min. Afterwards, the unreacted fluorescein molecules were removed by washing with distilled water. The samples were then placed in 3 mL of a 0.5% solution of hexadecyltrimethyl ammonium bromide to exchange

with the bounded fluorescein molecules under ultrasound for 15min. 0.45 mL of saturated NaHCO₃ solution was added after sonication. Then the absorbance of solution was recorded at 501 nm. The fluorescein concentration was then calculated using a calibration curve.

Antimicrobial activity assay (Live/Dead test)

A 130 µl droplet of *E. coli* or *S. epidermidis* suspension in distilled water (about 5×10^8 CFU/ml) was spread on the modified surfaces (1.8×1.8 cm²) using a glass slide with the same surface size for 1 h. Then the glass slide was taken away and the PDMS surfaces were washed by distilled water flow to remove the non-attached bacteria. After that, a 130 µl mixture of two fluorescent markers: the SYTO[®] and the propidium iodide, were deposited and spread on the surfaces for 15 min. The mixture was diluted prior to use (20 µmol/l of SYTO[®]9). Images (1024 × 1024 pixels) of surfaces were acquired using an upright fixed-stage Leica TCS SP8 CFS confocal microscope (Leica Microsystems, Nanterre, France) equipped with diodes laser (Coherent, Les Ulis, France) at 488 nm to excite the SYTO[®]9 and at 552 nm to excite Propidium Iodide and a conventional scanner at 400 Hz. Using a 63× oil immersion objective (1.40), fluorescence emission was sequentially detected through hybrid detector (Leica Microsystems, Nanterre, France) in photon counting mode with a specific band from 500 to 540 nm for SYTO[®]9 and 580 to 630 nm for Propidium Iodide. Z-Stack's images were acquired using an adapted step-size from Nyquist Criteria. ImageJ (Rasband W.S., U.S. National Institutes of Health, Bethesda, Maryland, USA, <http://imagej.nih.gov/ij/>, 1997-2020) was used to adjust brightness and contrast and to perform z projections of 3D images (xyz). **The Live and Dead test was performed on at least three independent samples, and two/three representative pictures by sample were recorded.**

Results and discussion

Phosphonium monomer was synthesized in three steps. First, a Diels-Alder adduct (exo-7-oxabicyclo[2.2.1]hept-5-ene-2,3-dicarboxylic anhydride) was obtained from maleic anhydride and furan. Then, imide transformation, in the presence of sodium acetate/acetic anhydride mixture, was performed with 3-bromopropylamine hydrobromide. This bromo oxanorbornene derivative was further reacted with triphenyl phosphine by nucleophilic addition route to afford a phosphonium bearing oxanorbornene monomer [33]. Similarly, pyridinium based monomer was prepared by reacting the previous Diels Alder adduct with

pyridin-3-ylmethanamine, in the presence of catalytic amount of sodium acetate. Then, the pyridine ring was reacted with hexyl bromide to afford a quaternary pyridinium salt [34].

The prepared cationic monomers were then used in the ROMP type polymerization to procure well-defined polymers with controlled molecular weight and dispersity (\mathcal{D}) close to 1. Polymers with a targeted number of average molecular weight of 10 000 g/mol were obtained by adjusting the catalyst concentration.

Chemical structures of monomers and polymers were confirmed by NMR techniques. Complete conversion from monomer to polymer was inspected by the whole disappearance of the monomer olefin proton peaks at 6.0–6.3 ppm and the appearance of polymer backbone olefinic broad proton signals at 5.1–5.6 ppm. Binding aryl carbon to phosphonium cation was detected at δ 118 ppm in the ^{13}C NMR spectrum. Phosphonium peak of the p(OPPh) was observed at 24.5 ppm in the spectra of ^{31}P NMR. Pyridinium based polymers showed the characteristic peak of the protons in alpha position to the ammonium group at 2.1 ppm in the ^1H NMR spectrum, while ^{13}C NMR analysis showed the corresponding methylene carbons at 39 ppm. The molecular weights of the homopolymers were calculated by ^1H NMR end group analysis [33, 34] which was close to the targeting theoretical M_n values of the polymers.

The photo-grafting initiated by benzophenone of the cationic polymers onto the PDMS surface was first tested without pretreatment. The PDMS films (Sylgard[®]184) prepared at the conventional ratio of PartA (curing agent)/PartB (base) = 1/10 and were totally cured. A drop of the cationic polymer solution (10 to 50wt% in methanol) was spread on the PDMS surface by covering it with a thin glass plate. The sample was then introduced in the UV conveyor for 1.55 s of UV exposure by passage. Despite varying the concentration of the polymer solution and the number of passages under UV (50 to 90) the direct polymer grafting on the PDMS surface was not efficient as suggested by the water contact angle (WCA), which was very close to the value of the untreated PDMS (Table 1, control 1), i.e. 108°.

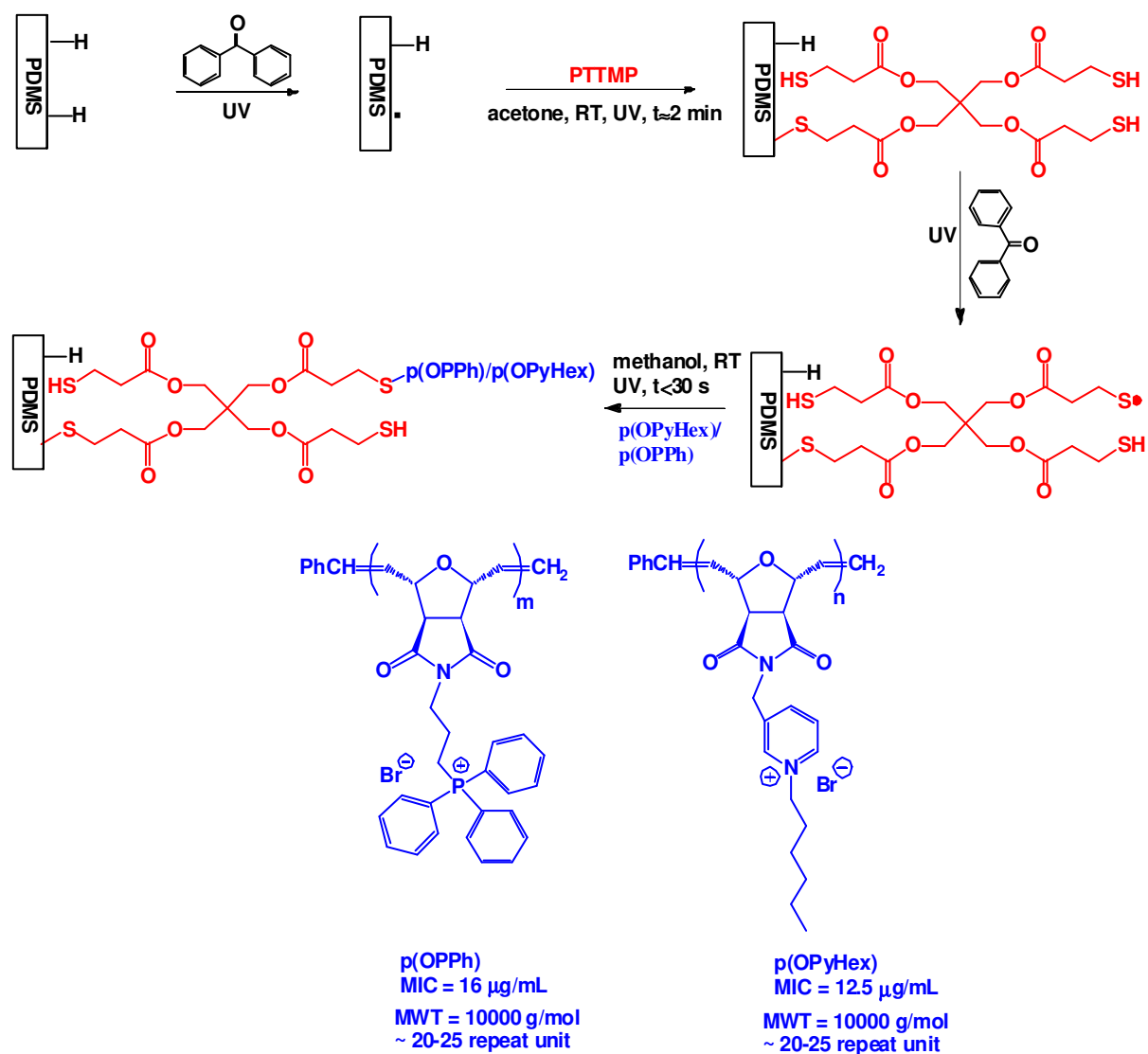


Figure 1. Photografting of p(OPPh) or p(OPyHex) onto PDMS surface with Pentaerythritol tetrakis (3-mercaptopropionate) (PTTMP) pretreatment.

Therefore, we have achieved a thiolation pretreatment of the PDMS surface to increase its reactivity (Figure 1). Indeed, radical sites can easily be formed from thiol groups under UV to achieve thiol-ene coupling reaction with the carbon-carbon double bonds of the polymers. Thus, a drop of solution of pentaerythritol tetrakis (3-mercaptopropionate) (PTTMP) in methanol was spread on the PDMS surface using a glass plate. The sample was disposed in the UV conveyor for several passages under UV. Various PTTMP concentration, ranged from 25 to 75wt%, and number of passages, ranged from 30 to 100, were tested. A constant value of the water contact angle of around 100° was obtained regardless the thiolation conditions (Table 1, control 3). For the next step, the thiolation was achieved with a solution of PTTMP at 50 wt% with 90 passages under UV, leading to the lowest standard deviation of the WCA value.

Then, the cationic polymers were grafted on the thiolated PDMS surfaces under UV at several exposure times and polymer concentrations. The optimal conditions were obtained for a polymer concentration of 10 wt% and a number of passages under UV of 15 leading to the most hydrophilic and functionalized surfaces, with WCA values of 78 and 98° for PDMS-T-p(OPyHex) and PDMS-T-p(OPPh) surfaces, respectively (Table 1). The difference in WCA values between the two surfaces can be ascribed to the higher hydrophobic character of the p(OPPh) compared to p(OPyHex), which is due to the number of carbons on these polymers (three phenyl groups versus one hexyl chain, respectively). This difference can also be partially ascribed to the overall surface coating efficiencies. Indeed, since the cationic polymers are hydrophilic and water soluble, increasing their grafting density would lead to an increase in surface hydrophilicity and a decrease of WCA.

Table 1. Data of contact angles measurements and surface charge densities on the optimal treated PDMS surface (10 wt% of polymer solution under UV, under 15 passages under UV) and their controls.

Samples	Static mode		Dynamic mode		Charge density	Roughness by AFM ^b (nm)	
	θ_{water} (°) ^a	AA (°) ^a	RA (°) ^a	Hyst (°) ^a	charge.cm ⁻²	Ra	RMS
PDMS (control 1)	108±2	116±3	58±4	57±2	ND	1.4	2.4
PDMS-T (control 2)	97±8	121±2	68±1	53±2	ND	2.8	3.7
PDMS-T-p(OPPh)	98±4	106±11	34±16	73±25	(4.8±1.1) ×10 ¹⁴	6.1	8.5
PDMS-T-p(OPyHex)	78±9	93±10	27±23	67±21	(3.2±0.5) ×10 ¹⁴	8.1	12.9

^a θ_{water} : contact angle with water; AA: Advancing Angle; RA: Receding Angle; Hyst: Hysteresis.

^b Ra: Arithmetic Average Roughness and RMS: Root Mean Square Roughness, from the 20×20 μm² images.

Measurements of the dynamic water contact angles were achieved on the optimal surfaces (Table 1). The advancing angle (AA) is correlated to the wettability of the hydrophobic parts of the surface while the receding angle (RA) is ascribed to the hydrophilic parts. Unmodified PDMS surfaces (control 1) exhibited values of AA, RA and the hysteresis (AA-RA) of 116°, 58° and 57°, respectively. The thiolated PDMS surface (control 2) showed

AA, RA and hysteresis values of 121°, 68° and 53°, respectively, confirming the success of the thiolation reaction. After treatment with the polymer solutions under UV, the modified surface showed a decrease of AA and RA to 106° and 34° for PDMS-T-p(OPPh) and to 93° and 27° for PDMS-T-p(OPyHex), respectively, suggesting a significant degree of surface grafting. However, the hysteresis increased to 73° and 63°, respectively, suggesting either a physical (roughness) and/or chemical (gradient of grafting density) gradients of the grafted surfaces.

The surface charge density is an important parameter that has been thoroughly used in the literature to predict the contact killing capacity of quaternary ammonium and quaternary phosphonium surfaces. Indeed, it has been established that the surface must own a minimal charge density value of 10^{14} charge.cm⁻² to kill quantitatively *E. coli* and *S. epidermidis* [23], [37]–[40]. The charge density values of the optimal cationic PDMS surfaces are displayed in Table 1. PDMS-T-p(OPPh) surface exhibited a charge density of $(4.8\pm 1.1)\times 10^{14}$ P⁺.cm⁻² whereas PDMS-T-p(OPyHex) showed a value of $(3.2\pm 0.5)\times 10^{14}$ N⁺.cm⁻² suggesting a high potential of bacterial killing of these prepared surfaces.

Surface characterization by AFM

AFM images of the prepared cationic surfaces and their controls are shown in Figure 2 and the supplementary information. One can observe structural and topographical variations on the PDMS surfaces after thiolation as well as after photo-grafting of the cationic polymers. The roughness values, from the 20×20 μm² images, of these modified and unmodified PDMS surfaces are presented in Table 1. The unmodified PDMS surface was very smooth with an arithmetic average roughness value of about 1.4 nm and a mean square roughness of about 2.4 nm (Figure 2-A, Table 1). White spots on this surface were rarely observed, which can be attributed to slight surface contamination by dust or particles from atmosphere or through manipulation with the clamp. The thiolated PDMS surface (PDMS-T) exhibited an increased roughness value around 2.8 nm and 3.7 nm, respectively (Figure 2-B, Table 1). PDMS-T-p(OPPh) surface (Figure 2-C, Table 1) exhibited roughness values around 6.1 nm and 8.5 nm whereas the roughness values of PDMS-T-p(OPyHex) (Figure 2-D, Table 1) were of 8.1 and 12.9 nm, respectively. However, both the two cationic surfaces showed the presence of polymer aggregates (white spots), which is often observed with the ‘grafting to’ method. Moreover, some big aggregates, of around 5 nm diameter, were observed on the PDMS-T-p(OPyHex) surface. However, some zones of this surface were quasi-empty of aggregates and

displayed roughness values of 0.6 and 1 nm, respectively, i.e. lower than those of PDMS-T. This result suggests that the p(OPyHex) was homogenously grafted on these zones.

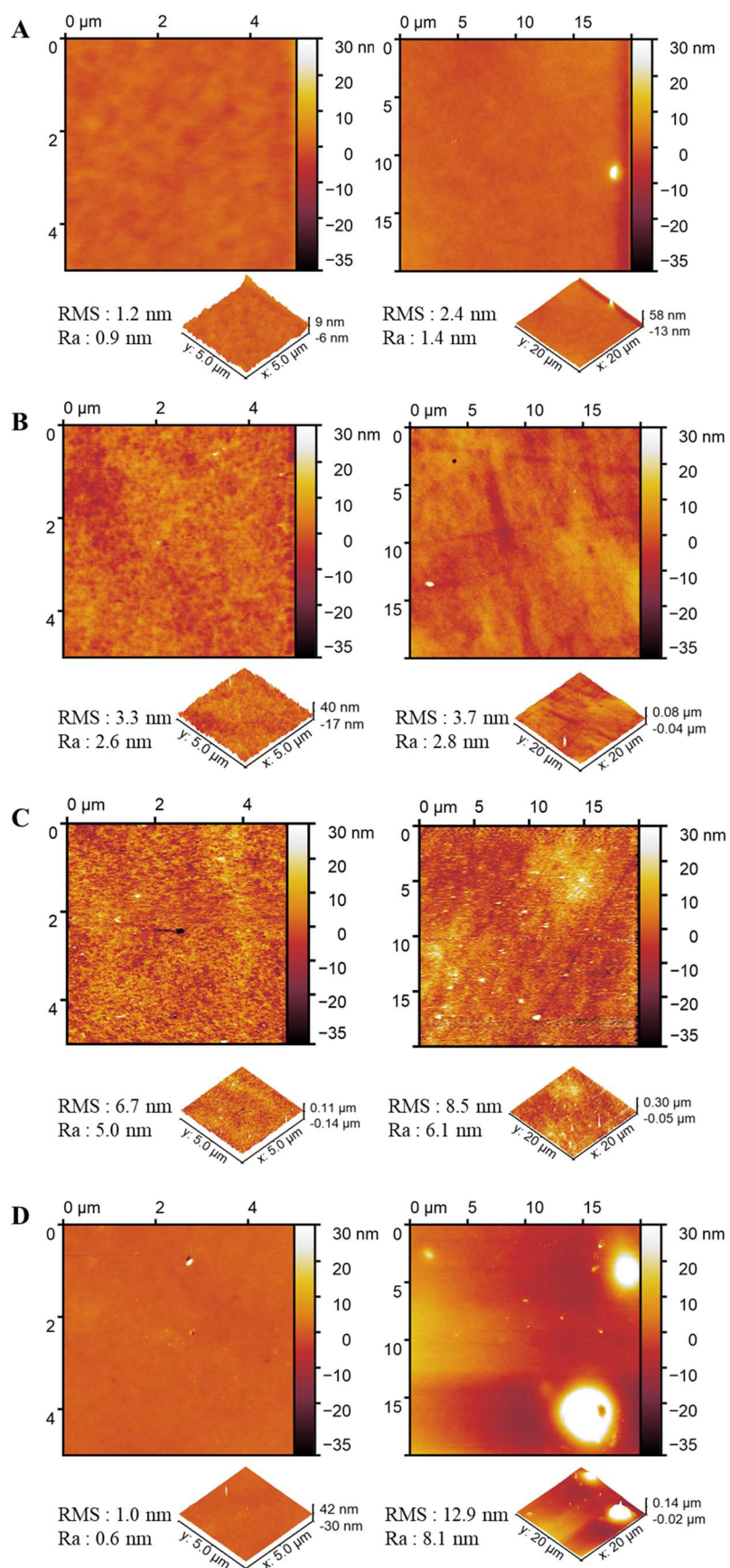


Figure 2. AFM images of (A) PDMS surface (control 1), (B) PDMS-T surface (control 3), (C) PDMS-T-p(OPPh) surface and (D) PDMS-T-p(OPyHex) surface.

The FTIR-ATR spectra of the prepared cationic surfaces, compared to their controls are shown in Figure 3. Zooms of the region between 1150 and 1900 cm^{-1} are given in the supporting information. The grafted PTTMP, which should form a very thin monomolecular layer, was not detected by this technique due to their weak amount on the surface. The PDMS-T-p(OPyHex) showed the appearance of a new band at around 1700 cm^{-1} arising from the stretching vibration of the carbonyl group of the imide function present in the grafted cationic polymer. One can observe also the stretching vibration band related to the polymer's carbon-carbon double bonds at 1636 cm^{-1} . A small band at 1503 cm^{-1} arising from the bending vibration of C-H in $\text{CH}_2\text{-N}^+$ groups was also observed. However, the characteristic bands corresponding to the imide function was not observed within the PDMS-T-p(OPPh) surface. This can be explained by the lower concentration of this function (~ 2 folds) within the p(OPPh). Moreover, the presence of big aggregates on the PDMS-T-p(OPyHex) surface may also be the **reason** of an increased signal intensity of the imide group in its FTIR spectrum. Anyway, these results suggest that the grafting density of p(OPyHex) on the surface was higher than the one of p(OPPh).

On the other hand, according to water contact angle results, PDMS-T-p(OPyHex) was more hydrophilic (78°) and more hygroscopic than the PDMS-T-p(OPPh) surface, which explain the appearance of a small band at 3300 cm^{-1} arising from the moisture in its FTIR spectrum.

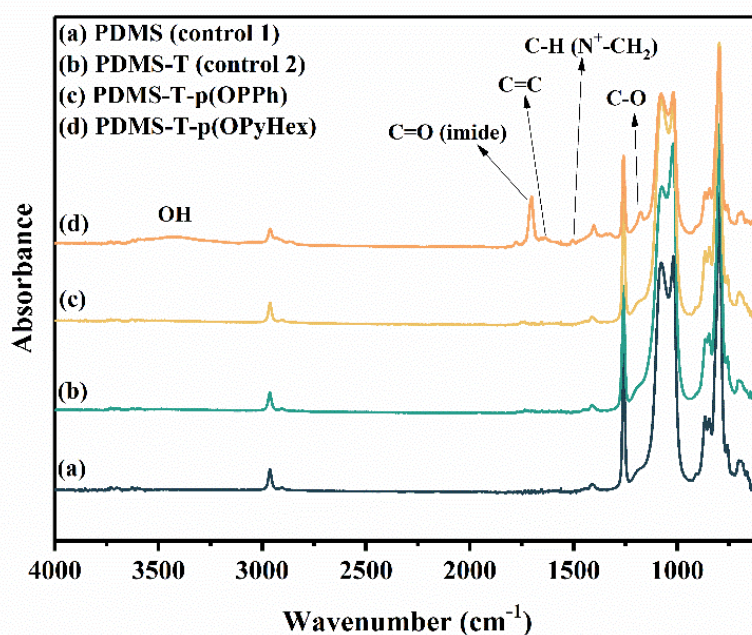


Figure 3. ATR-FTIR spectra of (a) PDMS (control 1), (b) PDMS-T (control 2), (c) PDMS-T-p(OPPh) and (d) PDMS-T-p(OPyHex).

The elemental analysis of the modified and unmodified PDMS surfaces was performed by XPS analysis. The results are presented in Table 2. The XPS analysis of the PDMS surface shows the presence of carbon, oxygen and silicon. A small enrichment of O and Si was observed for the native PDMS and could be explained by a residual SiO₂ coming from the synthesis process of the PDMS and also by the presence of residual Si-H groups after curing. After grafting of the PTTMP, peaks assigned to the sulfur element appear and an increase of the carbon amount was observed, confirming the presence of the grafted molecule on the surface.

Table 2. XPS elemental analysis of the optimal PDMS modified surface and its unmodified PDMS control.

	C1s	O1s	Si2p	N1s	P2p	Br3d	S2p	C/O	C/Si	O/Si	N/Br
PDMS	38.2	32.4	29.3	--	--	--	--	1.2	1.3	1.1	--
PDMS-T	47.1	28.3	22.9	--	--	--	1.7	1.7	2.1	1.2	--
PDMS-T-p(OPPh)	49.3	24	24.8	<0.3	<0.3	0.3	1.4	2.1	2.0	1.0	--
PDMS-T-p(OPyHex)	57.6	21.6	14.6	3.5	--	1.7	1	2.7	4.0	1.5	2

After grafting of p(OPPh) on the PDMS surfaces, a weak amount of Br was detected (0.3 at. %) with a decrease of sulfur amount, suggesting that the p(OPPh) was grafted on the surface. Unfortunately, the very weak amount of N and P (<0.3 at%) do not allow a fine quantification. This result can likely be explained by the ratios C/N and C/P equal to 21 in this polymer, conjugated to a partial coverage of the surface. Another aspect to consider is the π - π stacking between phenyl groups that may impact the relative accessibilities of P and Br atoms to the X-ray beam. Concerning the p(OPyHex), the ratio C/N and C/Br being equal to 10 and 20, respectively, N and Br elements of this polymer were detected with weak values (3.5 and 1.7%) and were in the expected stoichiometry (2/1). Thus, with regards to the surface elemental composition, the average grafting density is likely higher in the case of p(OPyHex) than in the case of p(OPPh). This can be explained by a lower concentration and accessibility of the carbon-carbon double bonds, **due to the steric hindrance of triphenyl unit**, as well as a lower solubility in methanol in the case of p(OPPh), leading to the decrease of its reactivity

towards the surface's thiol groups and the decrease of its grafting yield. The presence of big aggregates on the PDMS-T-p(OPyHex) surface may also explain this result.

Assessment of the surface bactericidal properties

Previously, we have demonstrated that phosphonium containing polynorbornenes (p(OPPh)) [41] and quaternary pyridinium functionalized polynorbornenes (p(OPyHex)) [42] have **strong** biocidal activities in solution against *Staphylococcus aureus* and *E. coli* respectively, with Minimal Inhibitory Concentrations (MIC) around 15 $\mu\text{g/mL}$. The bactericidal properties of p(OPPh) have also been evidenced in the solid state as a **non-grafted** coating on a glass surface [41]. **The ROMP based cationic pyridinium polymer with a hexyl unit exhibited the highest bactericidal efficiency in the solid state against *E. coli*, killing 99% of the bacteria in 5 min [42]. In addition, the introduction of phosphonium species at the polymer backbone would also increase its thermal stability. This would provide biocidal surface properties at high temperatures.**

The most common mechanisms for the bactericidal action of **cationic** surfaces suggest that the long cationic polymer chains infiltrate the cells and thus destroy the membrane, like a needle bursting a balloon. Since **cationic** surfaces with short polymer and alkyl chains have shown bactericidal effects, a second mechanism has been highlighted in the literature, suggesting an ion exchange between the positive charges of the surface and the divalent cations of the membrane, which are released from the cell. The loss of these structurally critical mobile cations leads to the destruction of the membrane [43].

The bactericidal properties of p(OPPh) and p(OPyHex) grafted onto PDMS surfaces were studied by the Live and Dead test, using confocal fluorescent microscopy, against *E. coli* (Gram-) and *S. epidermidis* (Gram+). Bacteria were dispersed on modified and unmodified PDMS surfaces during 1h. Then, they were stained with a mixture of SYTO 9 and propidium iodide as fluorescent probes that stained bacteria with damaged membrane in red and bacteria with intact membrane in green. Examples of the Live and Dead fluorescent images are shown in Figure 4. One can observe that both PDMS-T-p(OPyHex) and PDMS-T-p(OPPh) surfaces displayed a high bactericidal effect. Indeed, after 1h of contact with the cationic surfaces the quasi-totality (**>98%**) of adhered bacteria was red (Figure 4-A3, B3, A4 and B4). Moreover, the density of *E. coli* (Figure 4-A3 and A4) and *S. epidermidis* (Figure 4-B3 and B4) on the cationic surfaces was relatively high (around 10^5 cells/cm²). Oppositely, unmodified PDMS surfaces (controls 1 (PDMS) and 4 (PDMS-T)), didn't display any bacteria attachment after 1h of contact. This behavior has already been observed in our previous works [23, 37]. For

instance, PDMS surfaces grafted with poly(vinylbenzyl dimethylbutylammonium chloride) via the “grafting to” method exhibited 98 to 100% killing efficiency after 1h of contact with *E. coli* and *S. epidermidis*. The surface bacterial density ranged from 10^5 to 10^6 cell/cm² when the charge densities varied from 2×10^{14} to 1.2×10^{15} charge.cm⁻² [23]. **Actually, when bacteria have affinity with the surface, the increase of roughness would increase the bacterial adhesion because of the increase of the surface contact. However, in our case the difference of roughness between the cationic and non-cationic surfaces (controls: PDMS and PDMS-T) is not significant and *E. coli* and *S. epidermidis* have not affinity with the controls. Bacteria are allowed to sediment on the surfaces, after washing with water, they are totally removed from the hydrophobic control but are strongly adhered to the cationic surface owing to high attractive electrostatic interaction.**

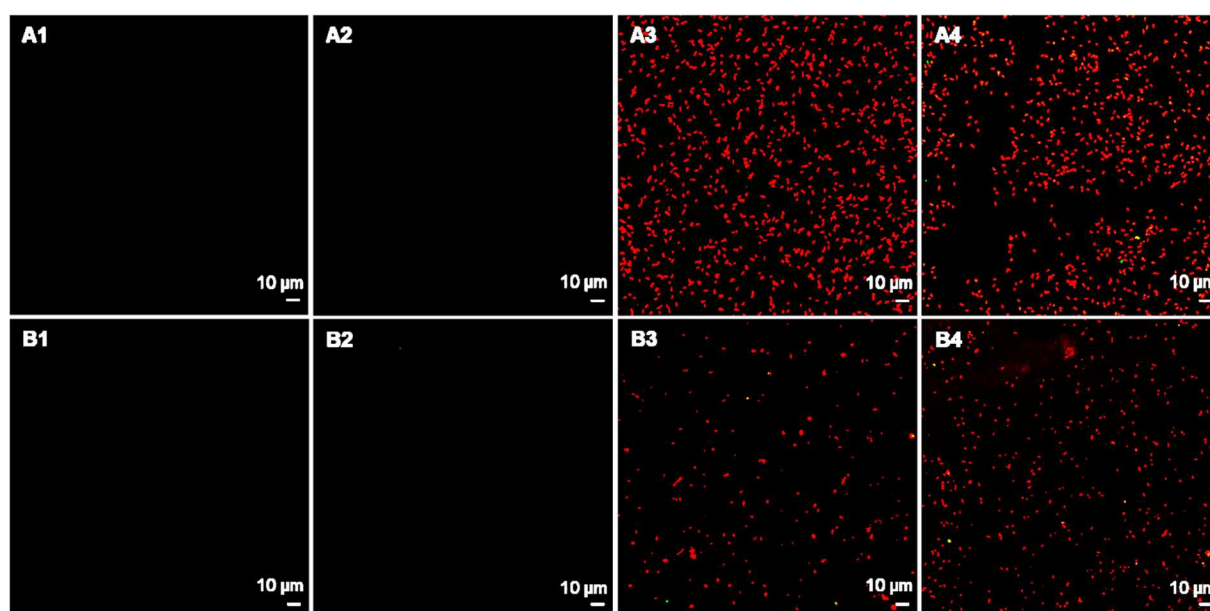


Figure 4. Fluorescence microscopy images of sessile bacteria cells stained with a marker of viability and deposited on surfaces of modified and unmodified PDMS surfaces: (A1) *E. coli* on unmodified PDMS surface (control 1), (A2) *E. coli* on PDMS-T surface (control 3), (A3) *E. coli* on PDMS-T-p(OPPh) surface, (A4) *E. coli* on PDMS-T-p(OPyHex) surface, (B1) *S. epidermidis* on unmodified PDMS surface (control 1), (B2) *S. epidermidis* on PDMS-T surface (control 3), (B3) *S. epidermidis* on PDMS-T-p(OPPh) surface, (B4) *S. epidermidis* on PDMS-T-p(OPyHex) surface.

In addition, a zone inhibition experiment was performed with *E. coli* and *S. epidermidis* on treated and untreated surfaces. Controls, consisting of PDMS-T surfaces on which the cationic polymers were deposited without UV exposure or subsequent washing, were also prepared. These controls showed a zone of inhibition with *S. epidermidis* but not with *E. coli*, which is usually less sensitive in this test. The grafted cationic surfaces did not show a zone of inhibition, suggesting that they are non-leaching.

The long-term biocidal activity of a cationic surface is essentially related to its charge density and also to the concentration of the bacteria exposed to it (the challenge). It has been demonstrated [43] that a cationic surface with a charge density greater than $5 \cdot 10^{15}$ charges/cm², is capable of killing at least a monolayer of *E. coli* cells (10^8 CFU/cm²), before undergoing fouling and losing its bioactivity. The live and dead test was performed with an extreme challenge of 1.5×10^8 CFU/cm² to achieve maximum bacterial adhesion on the surface leading to its saturation and passivation. Excess bacteria were washed away and the adherent bacteria (around 10^5 cells/cm²), thanks to the electrostatic forces promoted by the cationic charges, died. Under real conditions, extreme infection or contamination is reached when the bacterial concentration is about 10^3 CFU/cm². Therefore, the passivating bacterial concentration for our cationic surfaces (around 10^5 cells/cm²), can take a long time to be reached, depending on the number of bacteria to which these surfaces are exposed.

In previous studies, both p(OPPh) and p(OPyHex) have shown relatively high hemolytic activities in solution toward red blood mammalian cells [33,34]. In addition, we have also shown that cationic surfaces lost their bactericidal efficiency after 24 hours of contact with plasmatic proteins, which adsorbed easily on the surface by electrostatic attraction forces [23]. Therefore, at this time, we suggest to avoid the use of these surfaces in blood contact applications. On the other hand, they could be used for instance as external surface of catheter chambers and extracorporeal equipment.

Conclusion

Bactericidal cationic PDMS surfaces were successfully designed by a benzophenone photo-grafting process of ROMP-prepared cationic polymers. The grafting reaction was optimized in terms of duration and polymer concentration. The prepared surfaces exhibited surface charge densities above 10^{14} charge.cm⁻² and contact angle with water around 98° and 78° related to quaternary phosphonium and quaternary ammonium groups, respectively. The Live and Dead test by fluorescence microscopy revealed an efficient contact killing of these surfaces against *E. coli* and *S. epidermidis*. In the future studies, we intend to prepare analogue surfaces by developing a photo-initiated ROMP ‘grafting from’ method, which would result in higher surface grafting density and coverage as well as higher hydrophilicity. Recharge ability as well as biofilm formation on the passivated cationic surfaces will be investigated.

Acknowledgments

Authors thanks the INSA ROUEN NORMANDIE, Yildiz Technical University (Pr. Tarik EREN, project ID: FBA-2021-4120) and the China Scholarship Council (CSC) for the financial supports.

This manuscript is a tribute to the 50-year anniversary of the French Polymer Group (Groupe Français des Polymères - GFP).

Data availability statement

The raw/processed data required to reproduce these findings cannot be shared at this time due to technical or time limitations.

References

- [1] R. Yañez-Macías *et al.*, “Combinations of antimicrobial polymers with nanomaterials and bioactives to improve biocidal therapies,” *Polymers (Basel)*, vol. 11, no. 11, p. 1789, 2019.
- [2] U. S. D. of H. and H. Services, “CDC. Antibiotic Resistance Threats in the United States, 2019,” *Atlanta, GA, USA US Dep. Heal. Hum. Serv. CDC*, 2019.
- [3] N. M. Milović, J. Wang, K. Lewis, and A. M. Klibanov, “Immobilized *N* - alkylated polyethylenimine avidly kills bacteria by rupturing cell membranes with no resistance developed,” *Biotechnol. Bioeng.*, vol. 90, no. 6, pp. 715–722, 2005.
- [4] F. Siedenbiedel and J. C. Tiller, “Antimicrobial polymers in solution and on surfaces: overview and functional principles,” *Polymers (Basel)*, vol. 4, no. 1, pp. 46–71, 2012.
- [5] T.-F. Mah, B. Pitts, B. Pellock, G. C. Walker, P. S. Stewart, and G. A. O’Toole, “A genetic basis for *Pseudomonas aeruginosa* biofilm antibiotic resistance,” *Nature*, vol. 426, no. 6964, pp. 306–310, 2003.
- [6] G. J. Gabriel, A. Som, A. E. Madkour, T. Eren, and G. N. Tew, “Infectious disease: Connecting innate immunity to biocidal polymers,” *Mater. Sci. Eng. R Reports*, vol. 57, no. 1–6, pp. 28–64, 2007.
- [7] E. Klein, D. L. Smith, and R. Laxminarayan, “Hospitalizations and deaths caused by methicillin-resistant *Staphylococcus aureus*, United States, 1999–2005,” *Emerg. Infect. Dis.*, vol. 13, no. 12, p. 1840, 2007.
- [8] J. Yan *et al.*, “Cationic polyesters with antibacterial properties: facile and controllable synthesis and antibacterial study,” *Eur. Polym. J.*, vol. 110, pp. 41–48, 2019.
- [9] M. Alvarez-Paino *et al.*, “Antimicrobial surfaces obtained from blends of block copolymers synthesized by simultaneous atp and click chemistry reactions,” *Eur. Polym. J.*, vol. 93, pp. 53–62, 2017.
- [10] J. Velazco-De-La-Garza *et al.*, “Biological properties of novel polysuccinimide derivatives synthesized via quaternary ammonium grafting,” *Eur. Polym. J.*, vol. 131, p. 109705, 2020.
- [11] A. B. Swanson and L. F. Peltier, “Silicone Rubber Implants for Replacement of Arthritic or Destroyed Joints in the Hand.,” *Clin. Orthop. Relat. Res.*, vol. 342, pp. 4–

- 10, 1997.
- [12] M. Bračić, O. Šauperl, S. Strnad, I. Kosalec, O. Plohl, and L. F. Zemljič, “Surface modification of silicone with colloidal polysaccharides formulations for the development of antimicrobial urethral catheters,” *Appl. Surf. Sci.*, vol. 463, pp. 889–899, 2019.
- [13] A. Colas and J. Curtis, “Silicone biomaterials: history and chemistry,” *Biomater. Sci. an Introd. to Mater. Med.*, vol. 2, pp. 80–85, 2004.
- [14] A. U. Daniels, “Silicone breast implant materials,” *Swiss Med. Wkly.*, vol. 142, no. JULY, 2012.
- [15] K. W. Dunn, P. N. Hall, and C. T. K. Khoo, “Breast implant materials: sense and safety,” *Br. J. Plast. Surg.*, vol. 45, no. 4, pp. 315–321, 1992.
- [16] A. Colas, “Silicones: preparation, properties and performance,” *Dow Corning, Life Sci.*, 2005.
- [17] J. R. Henstock, L. T. Canham, and S. I. Anderson, “Silicon: the evolution of its use in biomaterials,” *Acta Biomater.*, vol. 11, pp. 17–26, 2015.
- [18] J. Winiecka-Krusnell and E. Linder, “Bacterial infections of free-living amoebae,” *Res. Microbiol.*, vol. 152, no. 7, pp. 613–619, 2001.
- [19] Q. Gao *et al.*, “Rationally designed dual functional block copolymers for bottlebrush-like coatings: In vitro and in vivo antimicrobial, antibiofilm, and antifouling properties,” *Acta Biomater.*, vol. 51, pp. 112–124, 2017.
- [20] A. I. Doulgeraki, P. Di Ciccio, A. Ianieri, and G.-J. E. Nychas, “Methicillin-resistant food-related *Staphylococcus aureus*: a review of current knowledge and biofilm formation for future studies and applications,” *Res. Microbiol.*, vol. 168, no. 1, pp. 1–15, 2017.
- [21] C. Donzel *et al.*, “Hydrophilic poly (dimethylsiloxane) stamps for microcontact printing,” *Adv. Mater.*, vol. 13, no. 15, pp. 1164–1167, 2001.
- [22] A. Oláh, H. Hillborg, and G. J. Vancso, “Hydrophobic recovery of UV/ozone treated poly (dimethylsiloxane): adhesion studies by contact mechanics and mechanism of surface modification,” *Appl. Surf. Sci.*, vol. 239, no. 3–4, pp. 410–423, 2005.
- [23] N. Kebir, I. Kriegel, M. Estève, and V. Semetey, “Preparation of bactericidal cationic

- PDMS surfaces using a facile and efficient approach,” *Appl. Surf. Sci.*, vol. 360, pp. 866–874, 2016.
- [24] W. Mussard, N. Kebir, I. Kriegel, M. Estève, and V. Semetey, “Facile and efficient control of bioadhesion on poly (dimethylsiloxane) by using a biomimetic approach,” *Angew. Chemie*, vol. 123, no. 46, pp. 11063–11066, 2011.
- [25] D.-J. Guo, H.-M. Han, S.-J. Xiao, and Z.-D. Dai, “Surface-hydrophilic and protein-resistant silicone elastomers prepared by hydrosilylation of vinyl poly (ethylene glycol) on hydrosilanes-poly (dimethylsiloxane) surfaces,” *Colloids Surfaces A Physicochem. Eng. Asp.*, vol. 308, no. 1–3, pp. 129–135, 2007.
- [26] Y. Wu, Y. Huang, and H. Ma, “A facile method for permanent and functional surface modification of poly (dimethylsiloxane),” *J. Am. Chem. Soc.*, vol. 129, no. 23, pp. 7226–7227, 2007.
- [27] H. Chen, Y. Chen, H. Sheardown, and M. A. Brook, “Immobilization of heparin on a silicone surface through a heterobifunctional PEG spacer,” *Biomaterials*, vol. 26, no. 35, pp. 7418–7424, 2005.
- [28] H. Chen, Z. Zhang, Y. Chen, M. A. Brook, and H. Sheardown, “Protein repellent silicone surfaces by covalent immobilization of poly (ethylene oxide),” *Biomaterials*, vol. 26, no. 15, pp. 2391–2399, 2005.
- [29] Y. Wang, H.-H. Lai, M. Bachman, C. E. Sims, G. P. Li, and N. L. Allbritton, “Covalent micropatterning of poly (dimethylsiloxane) by photografting through a mask,” *Anal. Chem.*, vol. 77, no. 23, pp. 7539–7546, 2005.
- [30] S. Sugiura, J. Edahiro, K. Sumaru, and T. Kanamori, “Surface modification of polydimethylsiloxane with photo-grafted poly (ethylene glycol) for micropatterned protein adsorption and cell adhesion,” *Colloids Surfaces B Biointerfaces*, vol. 63, no. 2, pp. 301–305, 2008.
- [31] B. L. Leigh, E. Cheng, L. Xu, A. Derk, M. R. Hansen, and C. A. Guymon, “Antifouling photograftable zwitterionic coatings on PDMS substrates,” *Langmuir*, vol. 35, no. 5, pp. 1100–1110, 2018.
- [32] Y. Lou, D. Schapman, D. Mercier, S. Alexandre, F. Burel, P. Thebault, N. Kébir. "Self-disinfecting PDMS surfaces with high quaternary ammonium functionality by direct surface photoinitiated polymerization of vinylbenzyltrimethylbutylammonium chloride,"

- Eur. Polym. J.*, vol. 152, pp. 110473, 2021.
- [33] N. C. Süer, C. Demir, N. A. Ünübol, Ö. Yalçın, T. Kocagöz, and T. Eren, “Antimicrobial activities of phosphonium containing polynorbornenes,” *RSC Adv.*, vol. 6, no. 89, pp. 86151–86157, 2016.
- [34] T. Eren *et al.*, “Antibacterial and hemolytic activities of quaternary pyridinium functionalized polynorbornenes,” *Macromol. Chem. Phys.*, vol. 209, no. 5, pp. 516–524, 2008.
- [35] A. Palantoken, M. S. Yilmaz, N. A. Unubol, E. Yenigul, S. Pişkin, and T. Eren, “Synthesis and characterization of a ROMP-based polycationic antimicrobial hydrogel,” *Eur. Polym. J.*, vol. 112, pp. 365–375, 2019.
- [36] H. S. Bazzi and H. F. Sleiman, “Adenine-containing block copolymers via ring-opening metathesis polymerization: synthesis and self-assembly into rod morphologies,” *Macromolecules*, vol. 35, no. 26, pp. 9617–9620, 2002.
- [37] J. Lafarge, N. Kebir, D. Schapman, and F. Burel, “Design of self-disinfecting PVC surfaces using the click chemistry,” *React. Funct. Polym.*, vol. 73, no. 11, pp. 1464–1472, 2013.
- [38] Y. Jiao, L. Niu, S. Ma, J. Li, F. R. Tay, and J. Chen, “Quaternary ammonium-based biomedical materials: State-of-the-art, toxicological aspects and antimicrobial resistance,” *Prog. Polym. Sci.*, vol. 71, pp. 53–90, 2017.
- [39] T. Zhou *et al.*, “Surface functionalization of biomaterials by radical polymerization,” *Prog. Mater. Sci.*, vol. 83, pp. 191–235, 2016.
- [40] J. C. Tiller, C.-J. Liao, K. Lewis, and A. M. Klibanov, “Designing surfaces that kill bacteria on contact,” *Proc. Natl. Acad. Sci.*, vol. 98, no. 11, pp. 5981–5985, 2001.
- [41] C. Demir *et al.*, “Biocidal activity of ROMP-polymer coatings containing quaternary phosphonium groups,” *Prog. Org. Coatings*, vol. 135, pp. 299–305, 2019.
- [42] E. Altay, M. A. Yapaöz, B. Keskin, G. Yucesan, and T. Eren, “Influence of alkyl chain length on the surface activity of antibacterial polymers derived from ROMP,” *Colloids Surfaces B Biointerfaces*, vol. 127, pp. 73–78, 2015.
- [43] H. Murata, R. R. Koepsel, K. Matyjaszewski, and A. J. Russell, “Permanent, non-leaching antibacterial surfaces-2: How high density cationic surfaces kill bacterial cells,”

Biomaterials, vol. 28, no. 32, pp. 4870–4879, 2007.

